Chemistry & Biology
Article

^{13}C-Flux Spectral Analysis of Host-Pathogen Metabolism Reveals a Mixed Diet for Intracellular *Mycobacterium tuberculosis*

Dany J.V. Beste,[1] Katharina Nöh,[2] Sebastian Niedenführ,[2] Tom A. Mendum,[1] Nathaniel D. Hawkins,[3] Jane L. Ward,[3] Michael H. Beale,[3] Wolfgang Wiechert,[2] and Johnjoe McFadden[1,*]
[1]Department of Microbial and Cellular Sciences, Faculty of Health and Medical Sciences, University of Surrey, Guildford GU2 7XH, UK
[2]Forschungszentrum Jülich, GmbH, IBG-1, Biotechnology and JARA-HPC, 52428 Jülich, Germany
[3]National Centre for Plant and Microbial Metabolomics, Rothamsted Research, Harpenden, Herts AL5 2JQ, UK
*Correspondence: j.mcfadden@surrey.ac.uk
http://dx.doi.org/10.1016/j.chembiol.2013.06.012

SUMMARY

Whereas intracellular carbon metabolism has emerged as an attractive drug target, the carbon sources of intracellularly replicating pathogens, such as the tuberculosis bacillus *Mycobacterium tuberculosis*, which causes long-term infections in one-third of the world's population, remain mostly unknown. We used a systems-based approach—^{13}C-flux spectral analysis (FSA) complemented with manual analysis—to measure the metabolic interaction between *M. tuberculosis* and its macrophage host cell. ^{13}C-FSA analysis of experimental data showed that *M. tuberculosis* obtains a mixture of amino acids, C_1 and C_2 substrates from its host cell. We experimentally confirmed that the C_1 substrate was derived from CO_2. ^{13}C labeling experiments performed on a phosphoenolpyruvate carboxykinase mutant revealed that intracellular *M. tuberculosis* has access to glycolytic C_3 substrates. These findings provide constraints for developing novel chemotherapeutics.

INTRODUCTION

Tuberculosis (TB) remains a major problem throughout the world and is responsible for 8.8 million cases of TB each year, resulting in 1.4 million deaths (World Health Organization, 2011). New drugs are urgently needed to combat the emergence of multidrug (MDR) and extensively resistant (XDR) TB (Sharma and Mohan, 2006; Velayati et al., 2009) strains of the pathogen. Intracellular metabolism of *M. tuberculosis* is an attractive target for development of novel anti-TB drugs; but despite more than a century of research, fundamental questions remain, such as the nature of the nutrients the pathogen obtains from its macrophage host cell. Mutagenesis studies (Muñoz-Elías and McKinney, 2005; Pandey and Sassetti, 2008) provide indirect evidence for a diet of fatty acids derived from host lipids, including cholesterol. However, definitive conclusions are compromised by the multiple roles of enzymes, the redundancy of metabolic pathways (Venugopal et al., 2011), and often contradictory data. More direct methods are therefore required to unravel the diet and metabolism of intracellular *M. tuberculosis*, which could illuminate novel treatment strategies against TB.

Recently, ^{13}C-isotopologue profiling analysis (^{13}C-IPA) based on mass spectrometry has been used to directly measure the intracellular metabolism of *Listeria monocytogenes* (Eisenreich et al., 2006) and several enterobacterial pathogens (Götz et al., 2010). This method involves using ^{13}C-labeled substrates (^{13}C-labeled substrates can either be provided during the infection or host cells can be labeled prior to infection) to track the intracellular metabolism of bacteria. The bacterial and host cells are then separated and the pattern of label in stable metabolites (proteinogenic amino acids) is measured using mass spectrometry. Model-free analysis is then used to infer the substrates transport reactions and central metabolic pathway utilization that are most consistent with the data. We previously applied the systems-based tool ^{13}C-metabolic flux analysis (^{13}C-MFA) (Wiechert et al., 2001) to directly measure metabolic fluxes of *M. tuberculosis* in vitro (Beste et al., 2011) and demonstrated the operation of an alternative pathway to the TCA cycle, the GAS pathway, which utilizes the Glyoxylate shunt and Anapleurotic reactions for oxidation of pyruvate, and Succinyl CoA synthetase for the generation of succinyl CoA and involves significant levels of CO_2 fixation. The method is based on similar principles to ^{13}C-IPA but uses in silico modeling to infer metabolic fluxes from the labeling patterns. Classical ^{13}C-MFA can only be applied to metabolic systems in steady state. Thus, to examine the non-steady-state metabolism of intracellular TB bacilli, we developed a systems-based tool—^{13}C-flux spectral analysis (^{13}C-FSA)—and applied it to investigate the diet and metabolism of intracellular *M. tuberculosis*.

RESULTS

Measuring the Intracellular Metabolism of *M. tuberculosis*

We used the THP-1 cell line as our model system for investigating the metabolic interaction between *M. tuberculosis* and

macrophages. Although human alveolar macrophages (HAM-M) are the natural host for *M. tuberculosis*, they can only be collected via an invasive medical procedure and are impossible to obtain in large enough numbers for systems biology-type studies. Peripheral blood mononuclear cell-derived macrophages (PBMC-M) have been used as an alternative, but there are significant limitations of using PBMC-M cells, including large heterogeneity between donors and even within the population of cells and variable ex vivo differentiation procedures (Martinez et al., 2006), and it is not possible to obtain enough PBMC's to perform the experiments presented here. THP-1 cells can be differentiated into macrophages following phorbol 12-myristate 13-acetate (PMA) stimulation and closely model the behavior of activated primary alveolar macrophage (Riendeau and Kornfeld, 2003) or peripheral blood mononuclear cell-derived macrophages (PMBC) following *M. tuberculosis* infection (Singhal et al., 2007). Differentiated THP-1 macrophages have been widely utilized as a model for *M. tuberculosis* infection in numerous studies, which furthered our knowledge on the interaction between *M. tuberculosis* and its host cell (for examples, see Kumar et al., 2010; Singh et al., 2012; Simeone et al., 2012; Fontán et al., 2008).

Human THP-1 macrophage-like cells were passaged three times in Roswell Park Memorial Institute (RPMI) media containing 100% uniformly labeled [U-$^{13}C_6$] glucose (^{13}Cglucose-RPMI), before the cells were differentiated into macrophages by stimulation with phorbol 12-myristate 13-acetate (PMA), also in ^{13}Cglucose-RPMI. After washing, the cells were infected with the H37Rv strain of *M. tuberculosis* (MOI = 5), incubated for 48 hr in unlabeled RPMI medium, and harvested. Differential centrifugation was used to separate cell lysates into intracellular bacterial and macrophage fractions. Cells were harvested at 48 hr as preliminary time course experiments demonstrated that *M. tuberculosis* was growing within macrophages at this time point (data not shown) and intracellular amino acids had attained a pseudoisotopic steady state (Table S1 available online). In parallel, control flasks of (1) uninfected labeled THP-1 cells and (2) *M. tuberculosis* were cultivated in ^{13}Cglucose-RPMI medium for 48 hr. After acid hydrolysis, the isotopomer (with the same molecular formula but different isotopic composition) composition of proteinogenic amino acids was measured using gas chromatography-mass spectrometry (GC-MS). Using this method, ten amino acids were isolated in sufficient quantities for accurate measurement of the ^{13}C enrichment. In the macrophage fraction, heavy isotopomer fractions (indicating incorporation of ^{13}C) were detected in the nonessential amino acids, but not the essential amino acids, as expected (Figure 1; Table S2). In contrast, in the intracellular bacterial fraction, all amino acids were labeled with ^{13}C. The distinct labeling patterns confirmed that differential centrifugation was successful in separating macrophage and intracellular *M. tuberculosis* fractions and demonstrated that the macrophages imported unlabeled (^{12}C) essential amino acids from the RPMI medium but made nonessential amino acids (incorporating ^{13}C) de novo, whereas *M. tuberculosis* amino acids were all synthesized from host-derived substrates (either de novo or directly incorporated from the host cell into protein). Perhaps surprisingly, there was no observed difference between the isotopologue profile of infected and uninfected macrophages (Table S2).

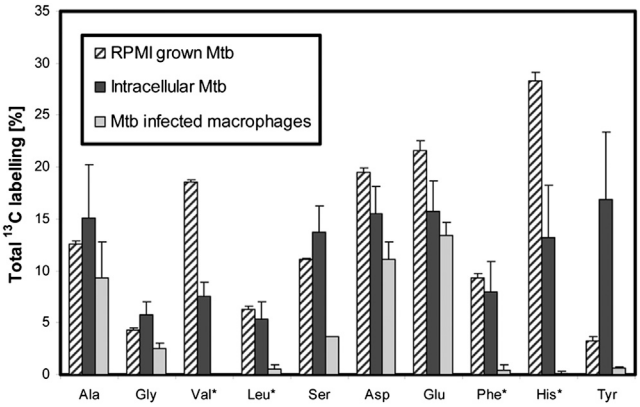

Figure 1. Total ^{13}C Labeling of Amino Acids Derived from Macrophages and *M. tuberculosis* Protein

GC-MS measured values for the total ^{13}C incorporation into proteinogenic amino acids by RPMI-grown *Mycobacterium tuberculosis* (MTB), intracellular MTB, and infected THP-1 macrophages after 48 hr. The THP-1 cells were prelabeled by passaging with uniformly labeled [U-$^{13}C_6$] glucose prior to the infections. Essential amino acids are indicated (*). Error bars indicate SD of triplicate or quadruplicate samples from independent macrophage infections. See also Table S1.

^{13}C-Flux Spectral Analysis

Because of the complexity of the data, we developed ^{13}C-flux spectral analysis (FSA) to perform unsupervised systems-level analysis of the isotopologue profiles using an in silico model of metabolism. ^{13}C-FSA utilizes similar fitting approaches as ^{13}C-MFA, essentially to find the best fit of different hypotheses of nutrient uptake by *M. tuberculosis* to the measured data. Inputs to ^{13}C-FSA are the isotopomer composition of macrophage amino acids (deconvoluted from the measured labeling patterns), the estimated isotopomer compositions of macrophage glucose, acetate, and glycerol pools (also obtained from the macrophage data and knowledge of the input $^{13}C_6$ glucose), and the *M. tuberculosis* labeling data. Various hypotheses for nutrient uptake by *M. tuberculosis* were then tested in automated simulations (more than 600,000 optimization runs) to identify substrates and flux distributions that minimized the "residual value", which is a measure of the quantity of the measured GC-MS data that could not be accounted for by the optimal in silico solution.

^{13}C-FSA was used to scan a range of potential substrates (glucose, glycerol, acetate, or single amino acids) and combinations of substrates, which *M. tuberculosis* may obtain from the macrophage. All single substrates generated high residual values (poor fit to data), as shown in Figure 2, but pairs of substrates that included acetate generated lower residual values, with acetate and alanine providing the best fit. Adding a third substrate to the combination of alanine and acetate (Figure 2, inset) resulted in small improvements to the fit with the lowest residual value obtained with serine. ^{13}C-FSA generated a flux solution with these substrates (Figure 3), which shares some features with the GAS pathway that we previously demonstrated operating in glycerol-limited chemostat-grown *M. tuberculosis* (Beste et al., 2011).

Manual inspection of the labeling profile confirmed many aspects of the ^{13}C-FSA solution. For instance, valine and alanine,

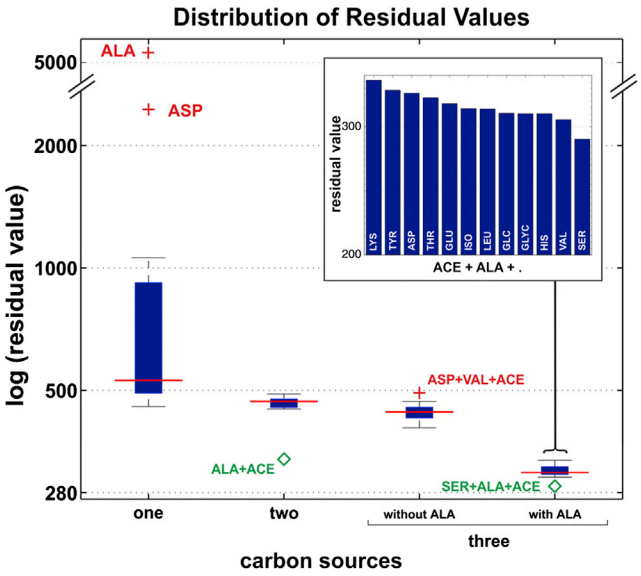

Figure 2. Box Plot Representation of the Log Residual Values Obtained by ^{13}C-FSA

Combinations of up to three intracellular carbon substrates were tested from 14 potential sources (alanine [ALA], acetate [ACE], glucose, glycerol, asparagine/aspartate [ASP], glutamate/glutamine [GLU], histidine [HIS], isoleucine [ISO], leucine [LEU], lysine [LYS], serine [SER], threonine [THR], tyrosine [TYR], and valine [VAL]). One and two carbon sources are represented by single bars, whereas three carbon sources are represented by two bars (with and without ALA). The inset histogram represents the logged residual values for combinations of three substrates, including ALA and ACE, showing that the optimal combination of substrates is ACE, ALA, and SER. The box plots depict the interquartile range (IQR) between the upper (Q3) and lower (Q1) quartiles (blue lines) and the median (red line). The length of the box represents the interquartile range (IQR). Whisker caps extend from the ends of the box within one IQR in each direction. Values more than one IQR from the upper whisker represent outliers, which are unlikely carbon sources (red cross), whereas values of less than one IQR from the lower whisker represent potential carbon substrates (green diamond) and are labeled with the name of the carbon source(s).

which are both formed from the same precursor (pyruvate), had discordant isotopomer profiles, indicating that they were not derived from the same precursor pool. The similarity between the composition of both bacterial and macrophage alanine (Figure 4A), but distinct patterns found for valine (Figure 4B), indicated that the *M. tuberculosis* alanine was directly imported from the macrophage, whereas valine was predominantly synthesized de novo in *M. tuberculosis*. The dominant isotope for both bacterial and macrophage alanine was M+3 (Figure 4A). In the macrophage, the metabolic precursor for $^{13}C_3$ alanine is $^{13}C_3$ pyruvate derived from [U-$^{13}C_6$] glucose. The ^{13}C isotopologue profile of intracellular *M.-tuberculosis*-derived valine (produced by two pyruvate molecules with the removal of one carbon atom by decarboxylation) (Figure 4B) indicated that this amino acid was not derived from $^{13}C_3$ pyruvate, owing to the absence of $^{13}C_5$ labeling. By comparison, the labeling of alanine in the control cells grown in ^{13}Cglucose-RPMI was predominantly $^{13}C_3$, and as expected, significant levels of $^{13}C_5$ valine were also detected. These data confirm that alanine was imported from the macrophage into *M. tuberculosis* and used for bacterial protein synthesis without any remodeling of the carbon skeleton. The lower but significant amounts of $^{13}C_1$ and $^{13}C_2$ alanine, however, indicate that, in addition to direct incorporation, some alanine is also synthesized de novo. The labeling profile of valine also indicates that $^{13}C_3$-labeled host pyruvate is not a major carbon source for intracellular *M. tuberculosis* (Figure 4).

Manual inspection of the isotopomer composition of asparagine/aspartate (ASP; the individual amino acids cannot be separated by GC-MS) and glutamate/glutamine (GLU) were indistinguishable between *M. tuberculosis* and macrophage fractions (Figures 4C and 4D), indicating that these amino acids were also imported from the host cell and incorporated directly into biomass.

CO_2 Fixation

Although most carbon flux in intracellular *M. tuberculosis* appeared to be derived from acetate, significant $^{13}C_1$ and $^{13}C_3$ isotopomer signals in several amino acids (Figure 5; Table S2) were inconsistent with an exclusive C_2 feed into central metabolism. A potential source for the C_1 signal could be the anaplerotic reactions (phosphoenolpyruvate carboxykinase [PEPCK]/malic enzyme [MEZ]/pyruvate carboxylase [PYC]) operating in the direction of oxaloacetate/malate to fix carbon from CO_2 as we previously demonstrated in vitro (Beste et al., 2011). Although the ^{13}C-FSA solution showed a net gluconeogenic (decarboxylating rather than carbon-fixing) flux through these reactions (Figure 3), this result does not exclude the possibility that one or more of the contributing reactions could be operating in the reverse (anaplerotic) direction. To test this hypothesis, we infected unlabeled THP-1 macrophages with *M. tuberculosis* in RPMI medium containing sodium [^{13}C] bicarbonate (^{13}Cbicarbonate-RPMI). In accordance with expectations, there was no incorporation of CO_2-derived ^{13}C label into amino acids extracted from macrophages, whereas there was significant ^{13}C incorporation into ten of the amino acids extracted from the intracellular *M. tuberculosis* fraction (Figure 6; Table S3), proving that *M. tuberculosis* fixes CO_2 carbon during intracellular growth. In contrast, control experiments in which *M. tuberculosis* was grown directly in ^{13}Cbicarbonate-RPMI showed significant ^{13}C labeling in only three amino acids (glycine, ASP, and GLU), and the ^{13}C excess was significantly lower than for intracellular *M. tuberculosis* (Table S3). These results demonstrated enhanced CO_2 fixation during intracellular growth and a wider distribution of CO_2-derived carbon throughout central metabolism as compared with in vitro growth.

The predominance of ^{13}C label from CO_2 in ASP, threonine, and methionine during intracellular growth suggests that the carbon-fixing reaction is one or more of the anaplerotic reactions that generate their common precursor, oxaloactetate. Although anaplerotic fixation of CO_2 could be performed by PEPCK, PYC, or MEZ, our previous in vitro experiments indicated that PEPCK was operating in the anaplerotic direction to fix CO_2 (Beste et al., 2011). CO_2 has also been found to induce the expression of the gene encoding PEPCK, *pck*A (Watanabe et al., 2011). To investigate whether PEPCK was fixing intracellular CO_2, we repeated the ^{13}C-bicarbonate labeling experiment in a *pck*A knockout (KO) strain (Marrero et al., 2010). The background strain for Δ*pck*A was Erdman, but control experiments detected no significant labeling differences between *M. tuberculosis* Erdman

and H37Rv. Control in vitro experiments were also performed in ^{13}C-bicarbonate-RPMI. Significant ^{13}C labeling occurred in only four amino acids from the intracellular PEPCK mutant (glycine, ASP, MET, and GLU). In addition, incorporation into these amino acids was 50% less than the ^{13}C enrichment measured for the same amino acids from the wild-type strain, indicating that whereas PEPCK was contributing to carbon fixation in *M. tuberculosis* ex vivo, it was not the sole enzyme involved (Figure 6; Table S3). The restriction of ^{13}C labeling in Δ*pck*A to TCA cycle-derived amino acids demonstrated that carbon flux from fixed CO_2 requires PEPCK to reach glycolysis- or pentose-phosphate-derived metabolites and confirmed the gluconeogenic role of this enzyme when *M. tuberculosis* is replicating within a macrophage.

C_3 Substrate

The significant C_3 signal in the labeling data (Figure 5; Table S2) could have been generated by combinations of C_1 and C_2 units derived from CO_2 and acetate but could also indicate the presence of an additional carbon source feeding into central metabolism. The previous demonstration that gluconeogenic flux of acetate was abolished in vitro in a PEPCK KO (Marrero et al., 2010), together with our results, which show that there is a similar block in macrophages, prompted us to use this strain to probe for additional glycolytic substrates. We performed intracellular ^{13}C isotopologue experiments with the PEPCK deletion mutant and respective parent Erdman strain using THP-1 macrophages that were prelabeled by passaging in ^{13}Cglucose-RPMI (Table S4), using an identical protocol to the experiments described for intracellular *M. tuberculosis* H37Rv. As a control, *M. tuberculosis* Erdman and ΔPEPCK were also grown for 48 hr in ^{13}Cglucose-RPMI media (Table S4). Again, we observed no significant difference between the profile of H37Rv and the Erdman strain of *M. tuberculosis*. These labeling experiments showed no significant differences in isotopomer composition between wild-type and Δ*pck*A for TCA cycle-derived amino acids, but in the case of amino acids derived from the pentose phosphate pathway and glycolysis/gluconeogenesis precursors (Figure 5; Table S4), there was a reduction in the $^{13}C_1$ and $^{13}C_2$ signal (presumably derived from acetate or CO_2) and retention of $^{13}C_3$ signal. The data clearly showed that, in addition to C_2 and C_1 substrates, *M. tuberculosis* is consuming substrate(s), which generate $^{13}C_3$ glycolytic intermediates. Moreover, the labeling profile indicates that this substrate is entering at the midpoint of the glycolytic/gluconeogenic pathway and then is primarily being channeled into the pentose phosphate pathway.

DISCUSSION

We (Beste et al., 2011) and others (de Carvalho et al., 2010) have demonstrated that *M. tuberculosis* cocatabolizes multiple carbon sources in vitro. Here, we show that intracellular *M. tuberculosis* also cocatabolizes several substrates, including amino acids, C_1, C_2, and C_3 substrates (Figure 7), a finding that has considerable implication for efforts to develop novel antituberculosis drugs that target substrate uptake or intracellular metabolism. The major carbon source feeding central metabolism was shown to be a C_2 compound that is highly likely to be acetate- or acetyl-CoA-derived from β-oxidation of host lipids, in agreement with previous indirect evidence (Muñoz-Elías and McKinney, 2005; Pandey and Sassetti, 2008) of a predominantly lipid diet for *M. tuberculosis* in vivo. However, our experiments with the PEPCK KO strain demonstrated that glycolytic C_3 compounds are also carbon sources for intracellular *M. tuberculosis*, as has been shown for intracellular *L. monocytogenes* (Eylert et al., 2010). The identity of these substrate(s) could be one or all of the amino acids that we demonstrated were imported by intracellular *M. tuberculosis*, e.g., alanine, glutamate/glutamine, or asparagine/aspartate. However, glycerol 3-phosphate (derived from abundant membrane phospholipids) or glycerol is also a potential C_3 source. Glycerol kinase, required for the conversion of glycerol to glycerol 3-phosphate, is dispensable for the growth of *M. tuberculosis* in a mouse model (Pethe et al., 2010), indicating that glycerol itself is not an essential carbon source.

M. tuberculosis auxotrophic mutants of leucine, proline, tryptophan, and glutamine have previously been shown to be severely attenuated in vivo (Lee et al., 2006; Smith et al., 2001; Hondalus et al., 2000; Tullius et al., 2003), indicating that biosynthesis of some amino acids is required in the intracellular environment; but several auxotrophic strains (e.g., methionine, isoleucine, and valine) can successfully proliferate in macrophages, indicating that other amino acids are acquired from the macrophage (Awasthy et al., 2009; McAdam et al., 1995). The data presented here showed that the macrophage amino acids alanine, glutamate/glutamine, and asparagine/aspartate were contributing to the intracellular nutrition of *M. tuberculosis*. Alanine is a critical structural component of peptidoglycan, and it has been shown that impairing the ability of *M. tuberculous* to convert L-alanine into D-alanine severely restricts intracellular growth, both in vivo and ex vivo in macrophages (Awasthy et al., 2009). By accessing host cell alanine pools, *M. tuberculosis* may ensure intracellular cell wall homeostasis. The data were also consistent with additional uptake of either glutamate and/or glutamine. *M. tuberculosis* has only limited access to glutamine within a phagosome, and a glutamine auxotrophic strain (*gln*A1 mutant) is highly attenuated in macrophages (Tullius et al., 2003). These results, together with our data, indicate that glutamate, rather than glutamine, is more likely to be the substrate derived from the macrophage. No data are available for *M. tuberculosis*-auxotrophic mutants of aspartate and asparagine. However, in a transposon screen mutations in genes involved in asparagine uptake (Rv2127 and Rv0346c) were shown to have decreased intracellular fitness (Stewart et al., 2005).

CO_2 is perhaps the most surprising carbon source demonstrated to be utilized by intracellular *M. tuberculosis* in this study. We previously established that glycerol-grown *M. tuberculosis* can incorporate CO_2 carbon into biomass in vitro (Beste et al., 2011), and this was also demonstrated in a hypoxic model of in vitro growth (Watanabe et al., 2011). The current study provides direct evidence that *M. tuberculosis* not only fixes CO_2 during intracellular growth but that fixation is at an increased level as compared with in vitro growth. The product of carbon fixation appears to be oxaloacetate generated partially, but not exclusively, by the action of PEPCK. The remainder of the CO_2 fixation could be performed by one or more of the anaplerotic reactions catalyzed by PYC and MEZ or via the activity

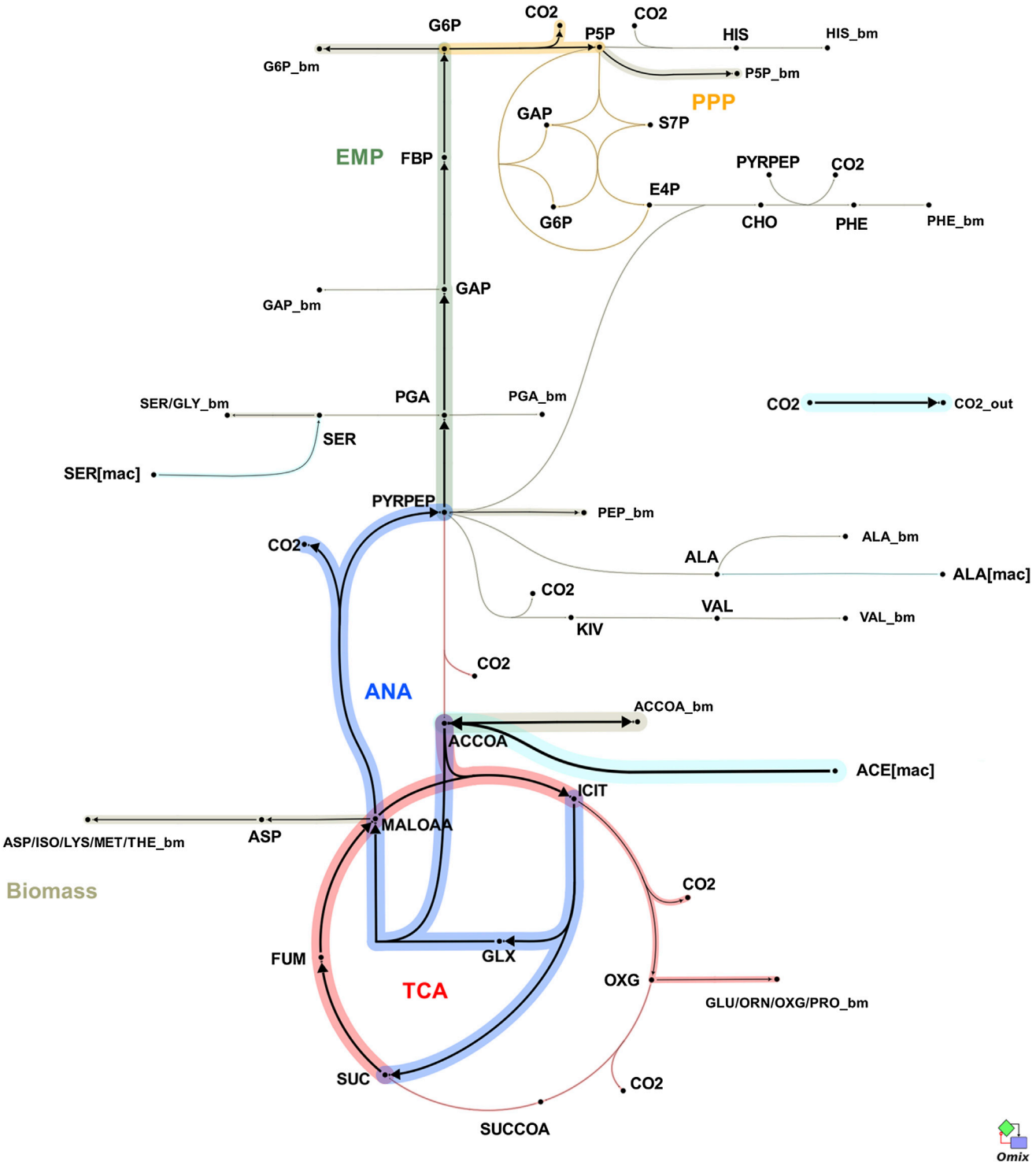

Figure 3. Estimated Carbon Flux Distribution through Central Metabolism for Intracellular *M. tuberculosis*

Arrows point in the net flux direction, and the width of each line is proportional to the underlying flux value. Glycolysis/gluconeogenesis (TCA), oxidative pentose phosphate pathway (EMP), tricarboxylic acid cycle (TCA), anaplerotic reactions (ANA). Standard abbreviations are used for the amino acids. Metabolite abbreviations: ACCOA, acetyl-CoA; ACE, acetate; CHO, chorismate; E4P, d-erythrose 4-phosphate; F6P, d-fructose 6-phosphate; FBP, d-fructose 1,6-bisphosphate; FUM, fumarate; G6P, d-glucose 6-phosphate; GA3P, glyceraldehyde 3-phosphate; GLX, glyoxylate; GLYC, glycerol; ICIT, isocitrate/citrate; KIV, 2-oxoisovalerate; MALOAA, l-malate-oxaloacetate; OXG, 2-oxoglutarate; R5P,α-d-ribose 5-phosphate/l-ribulose 5-phosphate/l-xylulose 5-phosphate; PEP, phosphoenolpyruvate; PGA, 2-phospho-d-glycerate/3-phospho-d-glycerate; PYR, pyruvate; S7P, sedoheptulose 7-phosphate; SUC, succinate; SUCCOA, succinyl-CoA. Enzyme abbreviations: CS, citrate synthase; ENO, enolase; FBA, fructose-bisphosphate adolase; FBP, fructose-bisphosphatase; FUM:fumurase;

(legend continued on next page)

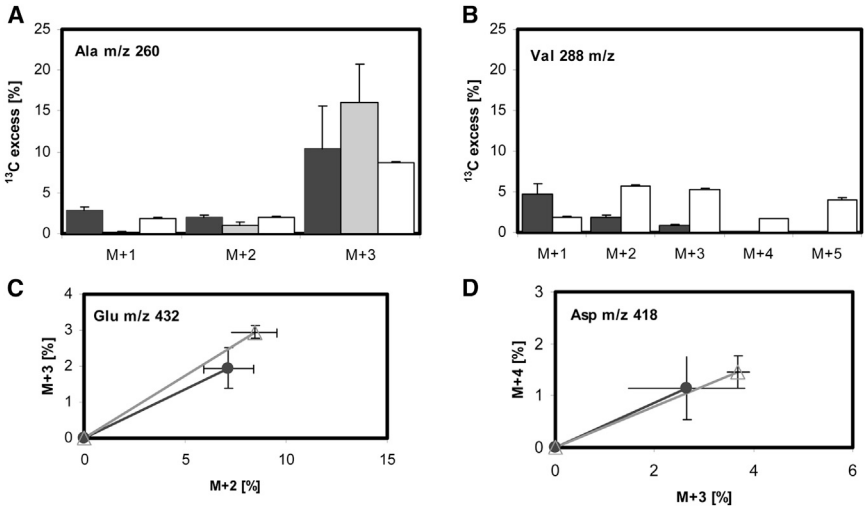

Figure 4. Isotopomer Profiles Indicate that Alanine, ASP, and GLU Are Predominantly Taken Up from Macrophages and Incorporated Directly into Biomass, whereas Valine Is Predominantly Synthesized De Novo

(A–D) Proportion of ^{13}C in isotopomers of alanine (A) and valine (B) derived from macrophage (gray bars), intracellular *M. tuberculosis* (black bars), and *M. tuberculosis* grown in labeled RPMI (white bars). Isotopomers ratios for GLU (C) and ASP (D) represented as line plots. The THP-1 cells were prelabeled by passaging with uniformly labeled [U-$^{13}C_6$] glucose prior to the infections. Closed symbols in black from intracellular *M. tuberculosis* protein; open symbols in gray from macrophage protein. The error bars indicate SD from 3–4 independent experiments.
See also Table S2.

of propionyl CoA carboxylase of the methylmalonyl pathway (MMP). MMP is one route for metabolizing propionyl CoA, which can be generated from oxidation of odd and branched chain fatty acids and cholesterol when sufficient amounts of vitamin B12 are present (Savvi et al., 2008). It has also been shown that MMP can provide an anaplerotic feed to the TCA cycle (Savvi et al., 2008). However, in previous studies supplementation of vitamin B12 was required to activate the MMP when *M. tuberculosis* was growing intracellularly (Griffin et al., 2012; Lee et al., 2013). The role of the methyl malonyl pathway in CO_2 fixation during intracellular growth is currently under investigation in our laboratory.

Cocatabolism of glucose, glycerol, and acetate in vitro has previously been reported to involve compartmentalized metabolism with each carbon source yielding distinct products (de Carvalho et al., 2010). Our data suggest a similar phenomenon operating inside macrophages, with the anaplerotic reactions operating in both the gluconeogenic (C_2 substrate) and carbon-fixing anaplerotic (C_3 substrate) direction simultaneously, despite the absence of a requirement for anaplerosis. It has previously been proposed that carbon fixation could play a role in maintaining redox balance in intracellular pathogens, acting as a redox sink in conditions of reduced oxygen availability (Srinivasan and Morowitz, 2006), a situation that may be relevant to the host environment of the TB bacillus. Carbon fixation provides a potentially attractive drug target, because macrophage cells are unable to fix CO_2.

Overall, these studies describe the direct measurements of nutrient uptake and metabolism of *M. tuberculosis* growing inside its host macrophage. This was facilitated by the development of ^{13}C-FSA, a powerful systems-based tool with utility in unraveling the complex metabolic interactions between host cells and their intracellular residents. The knowledge that *M. tuberculosis* cometabolizes a mixture of glycolytic and gluconeogenic carbon sources within a macrophage can be exploited in the design of suitable in vitro media for high-throughput drug screens, in addition to having implications for designing drugs that target nutrient uptake or intracellular metabolism of this and other intracellular pathogens.

SIGNIFICANCE

Tuberculosis (TB) is a disease that plagued ancient Egyptians and remains one of the biggest killers in the world today. A key to the success of *Mycobacterium tuberculosis*, the bacterium that causes TB, is its ability to survive and grow in macrophages, the very cells that are equipped to eliminate bacteria from the body. In order to do this, *M. tuberculosis* has to acquire nutrients and energy from this isolated niche. Several studies have highlighted the fact that targeting nutrient utilization is a potentially productive route for drug development, yet the nutrients consumed by intracellular *M. tuberculosis* are currently unknown. We used ^{13}C-labeled carbon sources to directly measure the metabolism of *M. tuberculosis* growing in macrophage host cells. Our data were analyzed using a bespoke mathematical model, which allowed us to identify that amino acids, C_1 and C_2 carbon sources were being obtained and metabolized by *M. tuberculosis* in the host cell. We have directly measured the intracellular metabolism of *M. tuberculosis* inside its host cell and used a mathematical approach—^{13}C-flux spectral analysis (^{13}C-FSA)—to scrutinize this type of complex interaction. We confirmed independently that the source of the C_1 substrate was CO_2. Using a mutant strain, we also demonstrated that C_3 substrates were also contributing to the intracellular diet of *M. tuberculosis*. These studies demonstrate that *M. tuberculosis* has access to a diverse diet within its host cell, a finding which has

GAPA, glyceraldehyde 3-phosphate dehydrogenase; GND, 6-phosphogluconate dehydrogenase; ICL, isocitrate lyase; ICDH, isocitrate dehydrogenase NADP-dependent; KOR/KGD, α-ketoglutarate ferredoxin oxidoreductase/α-ketoglutarate decarboxylase; MEZ/PCA, malic enzyme/pyruvate carboxylase: MDH, malate dehydrogenase; MS, malate synthase; PCK, phosphoenolpyruvate carboxykinase; PDH, pyruvate dehydrogenase; PGI, glucose phosphate isomerase; PYK, pyruvate kinase; SDH, succinate dehydrogenase; SCS, Succinyl CoA synthetase; TAL, transaldolase; TKT1/2, transketolase. Import from the macrophage is denoted as [mac], and export to biomass is labeled _bm.

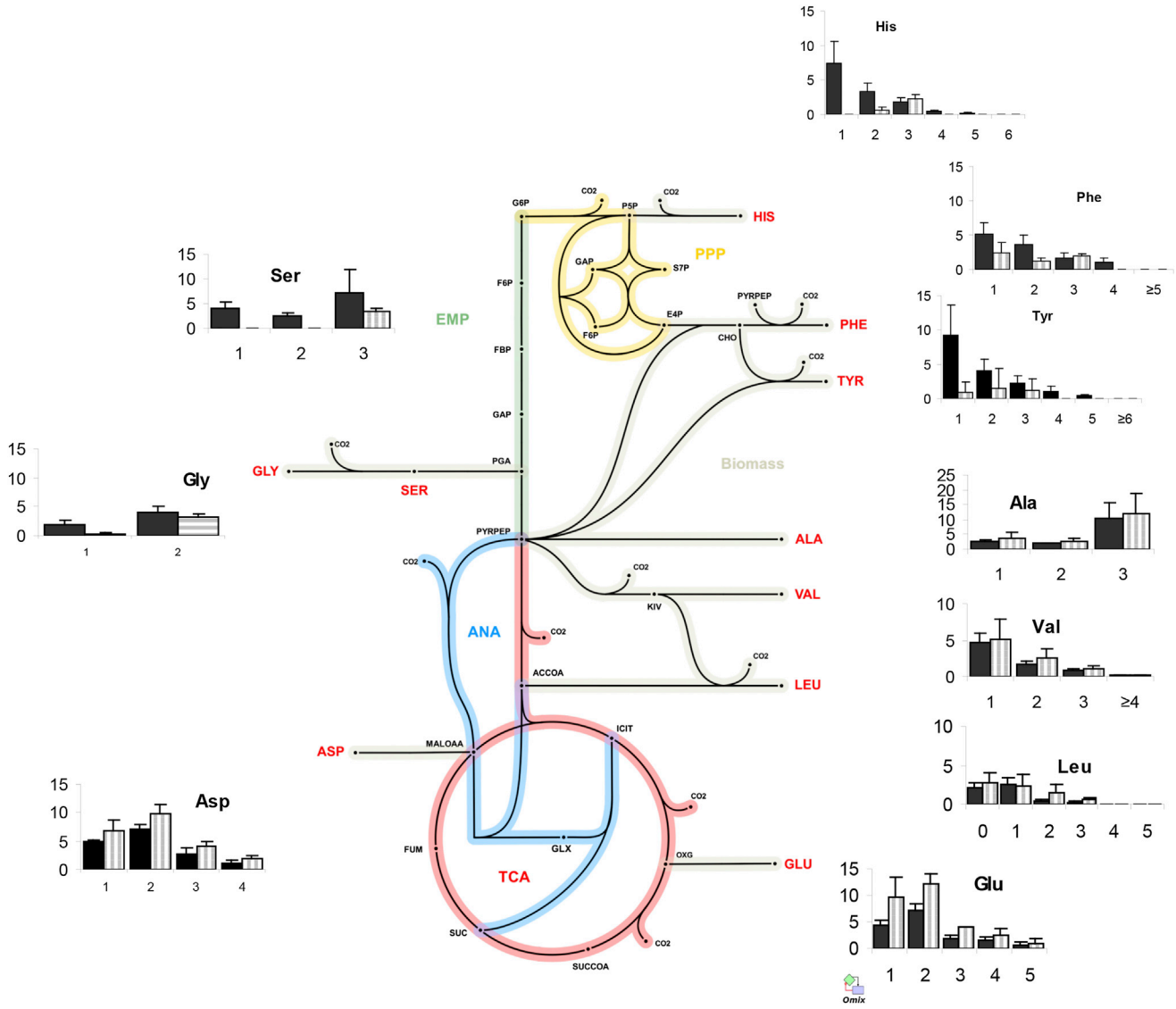

Figure 5. ^{13}C Isotopomer Distribution of Intracellular WT and ΔPEPCK *M. tuberculosis* Demonstrates Intracellular Consumption of Substrate(s), which Generate Significant $^{13}C_1$ and $^{13}C_3$ Intermediates

^{13}C isotopomer distribution after infection of THP-1 macrophages prelabeled (with [U-$^{13}C_6$] glucose) with wild-type (black bars) and ΔPEPCK (striped bars) *M. tuberculosis* superimposed on a metabolic network of central metabolism with the positioning of each chart indicating the source of the carbon backbone of each amino acid. Error bars indicate SD of 3–4 samples from independent macrophage infections.
See also Table S4.

significant implications for designing drugs against this and other intracellular pathogens, as well as advancing our knowledge of the pathogenesis of this globally important pathogen. We also describe an automated systems-level approach, which has utility in probing the intracellular metabolism of any microbe within their host cell.

EXPERIMENTAL PROCEDURES

Bacterial Strains and Growth Conditions

Frozen stock of *M. tuberculosis* was cultivated using Middlebrook7H11 agar and Middlebrook 7H9 broth containing 5% (v/v) oleic acid-albumin-dextrose-catalase enrichment medium supplement (Becton Dickenson) and 0.5% (v/v) glycerol. The knockout strain of *M. tuberculosis* Erdman PCK and the parent Erdman strain (Marrero et al., 2010) were kindly provided by Sabine Erht.

Cultivation of Human THP-1 Macrophages

The THP-1 human monocytic cell line was obtained from ATCC TIB-202. Cells were grown in RPMI 1640 medium supplemented with 0.2% glucose, 0.2% sodium bicarbonate, and 10% heat-inactivated fetal calf serum (Sigma). Labeled RPMI medium was prepared from RPMI without glucose or sodium bicarbonate (Sigma) by the addition of 100% [U-$^{13}C_6$] glucose and unlabeled sodium bicarbonate (Cambridge Isotope Laboratories), followed by sterile filtration. For the generation of ^{13}C-labeled THP-1 cells, RPMI media was prepared using 100% [U-$^{13}C_6$] glucose. Prelabeled monocytes were then generated by passaging the cells three times

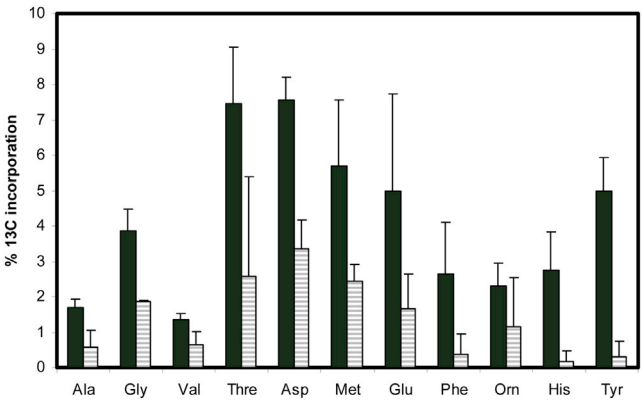

Figure 6. Intracellular *M. tuberculosis* Utilizes Carbon from Fixed CO_2, and the Enzyme PEPCK Is Contributing to the Observed Carbon Fixation

^{13}C-incorporation into proteinogenic amino acids by wild-type *M. tuberculosis* (black bars) and ΔPEPCK (striped bars) after 48 hr of growing intracellularly within THP-1 macrophages in the presence of sodium [^{13}C] bicarbonate. Error bars indicate SD of 3–4 samples from independent macrophage infections. See also Table S3.

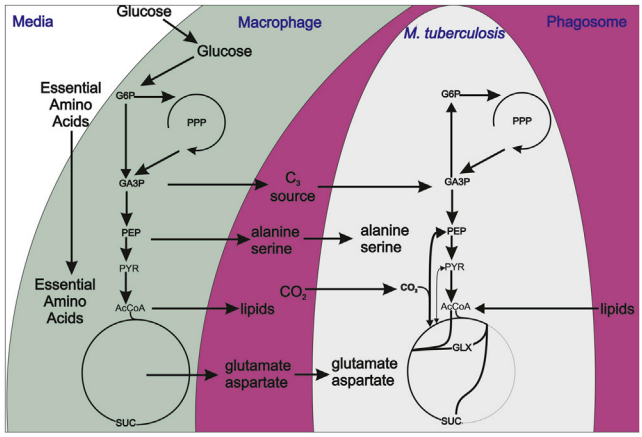

Figure 7. Substrates Consumed and Proposed Metabolic Pathways Employed by *M. tuberculosis*, Replicating in Macrophages

(12 days) in this media. RPMI was also prepared containing 0.2% sodium [^{13}C]bicarbonate (Cambridge Isotope Laboratories) for the carbon fixation experiments. Cultures were passaged twice a week and maintained at a density below 10^6 cells ml^{-1}.

Infection of Macrophages with *M. tuberculosis*

Bacterial infections were performed in 6–10 flasks (175 cm^2). Each flask was seeded with 3 × 10^7 THP-1 cells and differentiated with 50 nM PMA for 72 hr at 37°C, 5% CO_2, and 95% humidity. Cells were washed with PBS supplemented with 0.49 mM $Mg2^+$ and 0.68 mM $Ca2^+$ (PBS^+). *M. tuberculosis* cultures were grown exponentially in 7H9 liquid medium to an optical density of 1.0 (1 × 10^8 CFU ml^{-1}) for the infection and then washed in PBS and resuspended in RPMI with 20% FCS to obtain a bacterial suspension of 1.5 × 10^8 CFU ml^{-1}. A total of 1 ml of bacterial suspension was added to each flask (multiplicity of infection: five) and incubated for 3–4 hr. After incubation the macrophages were washed three times with PBS^+ and 30 ml of RPMI, plus 20% FCS was added to each flask. After incubation for 48 hr the floating cells were harvested by centrifugation at 300 × g for 5 min at 4°C. The adhered and floating cells were then washed with ice-cold PBS before being lysed with 0.1% Triton X-100. Mammalian cell debris was pelleted by centrifugation at 300 × g at 4°C. The supernatant containing the intracellular *M. tuberculosis* and the soluble host material was centrifuged at 4,000 × g for 20 min at 4°C to pellet the bacteria. The resulting supernatant was stored as a probe for the analysis of host cell amino acids. The resulting bacterial pellet was washed twice in RIPA buffer (Sigma) and was used as a probe for the analysis of ^{13}C labeling of amino acids in intracellular *M. tuberculosis*.

^{13}C Biomass Hydrolysate and Preparation of Amino Acid Derivatives

Amino acid derivatives were prepared from bacterial and host cell fractions as previously described (Beste et al., 2011). ^{13}C excess and the isotopologue composition was determined using GC-MS analysis as previously described (Beste et al., 2011). ^{13}C isotopologue abundances (i.e., ^{13}C incorporation; $^{12}C_n$, $^{13}C_1$, …, $^{13}C_n$) for each amino acid were determined for fragments containing the intact carbon skeleton for each amino acid, generally using the $[M-57]^+$ ion mass spectra of the derivatized amino acids. These were corrected for the natural abundance of all stable isotopes.

Network Model

An isotopomer model of the central metabolism of *M. tuberculosis* (Beste et al., 2011) was modified to include 11 amino acids, acetate (ACE), glycerol (GLYC), and glucose (GLC) as potential carbon exchange pools (Table S5). Exchange of carbon between the macrophage environment and *M. tuberculosis* was modeled via unidirectional reaction routes. A biomass formula (Beste et al., 2007) was introduced to constrain metabolic flux rates. In total, 55 intracellular reactions (25 unidirectional, 11 reversible) and 43 metabolites were subject to 14 possible uptake fluxes in the model (Table S3). Flux rates (total of 33) were estimated using a total of 120 measured GC-MS isotopomer/ isotopologue measurements (Table S6). For each combination of potential carbon source, a network variant was built. In order to make simulation results comparable among these model variants, the sum of all carbon uptake fluxes was normalized to one (= 100%), as the ratio between biomass formation and carbon uptake is not known for intracellular *M. tuberculosis*.

^{13}C-Flux Spectral Analysis

In order to reveal potential carbon sources (as isotopomers) for the intracellular mycobacterial cell, a multistage sampling-based ^{13}C-MFA-type approach was implemented. First, the measured labeling patterns of macrophage amino acids were deconvoluted by generating random isotopomer labeling patterns for each potential substrate imitating the measured isotopologues. If necessary, the direction of transport fluxes was modified from a nominal efflux to a nominal uptake flux. Because of stoichiometric constraints, additional flux directions were also adapted to guarantee a nonempty flux solution space. Second, multistart flux estimations were run based on initial flux space sampling as described elsewhere (optimization library: NAG C; [http://www.nag.co.uk] with flux sampling rate = 100 and maximal iteration number max_iter = 150; Dalman et al., 2013) to account for locality pitfalls of the nonlinear weighted least-squares fitting problem. Results for all measured isotopologues and initial and optimal flux distributions were recorded and ranked using the residual valine, and the best 100 flux fits (lowest residual valine) were selected for further analysis. Combinations of up to three carbon sources were rigorously analyzed in a large-scale computational study (in excess of 600,000 optimization runs) performed with the high-performance software 13CFLUX2 (Weitzel et al., 2013).

Statistical Analysis

Statistical analysis was performed using the Statistics Toolbox in Matlab 2001b (The Mathworks), and flux maps were visualized using Omix (v. 1.5.8, http://www.13cflux.net/omix). Best flux estimates were calculated by minimizing the sum of squares (residual values) of the offsets between the measured and simulated labeling patterns. Flux estimations, including the calculation of residual valine, were performed using 13CFLUX2 module *multifitfluxes* compiled for openSUSE 11.4 64bit (http://www.13cflux.net).

SUPPLEMENTAL INFORMATION

Supplemental Information includes six tables and can be found with this article online at http://dx.doi.org/10.1016/j.chembiol.2013.06.012.

ACKNOWLEDGMENTS

We thank Sabine Erht for the PEPCK KO strain and Michael Weitzel for providing customized 13CFLUX2 scripts. This work was supported by a grant from the Wellcome Trust (088677). The funders had no role in study design, data collection and analysis, decision to publish, or preparation of the manuscript.

Received: May 31, 2013
Revised: June 25, 2013
Accepted: June 26, 2013
Published: August 1, 2013

REFERENCES

Awasthy, D., Gaonkar, S., Shandil, R.K., Yadav, R., Bharath, S., Marcel, N., Subbulakshmi, V., and Sharma, U. (2009). Inactivation of the ilvB1 gene in *Mycobacterium tuberculosis* leads to branched-chain amino acid auxotrophy and attenuation of virulence in mice. Microbiology *155*, 2978–2987.

Beste, D.J., Hooper, T., Stewart, G., Bonde, B., Avignone-Rossa, C., Bushell, M.E., Wheeler, P., Klamt, S., Kierzek, A.M., and McFadden, J. (2007). GSMN-TB: a web-based genome-scale network model of *Mycobacterium tuberculosis* metabolism. Genome Biol. *8*, R89.

Beste, D.J.V., Bonde, B., Hawkins, N., Ward, J.L., Beale, M.H., Noack, S., Nöh, K., Kruger, N.J., Ratcliffe, R.G., and McFadden, J. (2011). ^{13}C metabolic flux analysis identifies an unusual route for pyruvate dissimilation in mycobacteria which requires isocitrate lyase and carbon dioxide fixation. PLoS Pathog. *7*, e1002091.

Dalman, T., Dörnemann, T., Juhnke, E., Weitzel, M., Wiechert, W., Nöh, K., and Freisleben, B. (2013). Cloud MapReduce for Monte Carlo bootstrap applied to Metabolic Flux Analysis. Future Gener. Comput. Syst. *29*, 582–590.

de Carvalho, L.P., Fischer, S.M., Marrero, J., Nathan, C., Ehrt, S., and Rhee, K.Y. (2010). Metabolomics of *Mycobacterium tuberculosis* reveals compartmentalized co-catabolism of carbon substrates. Chem. Biol. *17*, 1122–1131.

Eisenreich, W., Slaghuis, J., Laupitz, R., Bussemer, J., Stritzker, J., Schwarz, C., Schwarz, R., Dandekar, T., Goebel, W., and Bacher, A. (2006). ^{13}C isotopologue perturbation studies of *Listeria monocytogenes* carbon metabolism and its modulation by the virulence regulator PrfA. Proc. Natl. Acad. Sci. USA *103*, 2040–2045.

Eylert, E., Herrmann, V., Jules, M., Gillmaier, N., Lautner, M., Buchrieser, C., Eisenreich, W., and Heuner, K. (2010). Isotopologue profiling of Legionella pneumophila: role of serine and glucose as carbon substrates. J. Biol. Chem. *285*, 22232–22243.

Fontán, P., Aris, V., Ghanny, S., Soteropoulos, P., and Smith, I. (2008). Global transcriptional profile of *Mycobacterium tuberculosis* during THP-1 human macrophage infection. Infect. Immun. *76*, 717–725.

Götz, A., Eylert, E., Eisenreich, W., and Goebel, W. (2010). Carbon metabolism of enterobacterial human pathogens growing in epithelial colorectal adenocarcinoma (Caco-2) cells. PLoS ONE *5*, e10586.

Griffin, J.E., Pandey, A.K., Gilmore, S.A., Mizrahi, V., McKinney, J.D., Bertozzi, C.R., and Sassetti, C.M. (2012). Cholesterol catabolism by *Mycobacterium tuberculosis* requires transcriptional and metabolic adaptations. Chem. Biol. *19*, 218–227.

Hondalus, M.K., Bardarov, S., Russell, R., Chan, J., Jacobs, W.R., Jr., and Bloom, B.R. (2000). Attenuation of and protection induced by a leucine auxotroph of *Mycobacterium tuberculosis*. Infect. Immun. *68*, 2888–2898.

Kumar, D., Nath, L., Kamal, M.A., Varshney, A., Jain, A., Singh, S., and Rao, K.V.S. (2010). Genome-wide analysis of the host intracellular network that regulates survival of *Mycobacterium tuberculosis*. Cell *140*, 731–743.

Lee, S., Jeon, B.Y., Bardarov, S., Chen, M., Morris, S.L., and Jacobs, W.R., Jr. (2006). Protection elicited by two glutamine auxotrophs of *Mycobacterium tuberculosis* and in vivo growth phenotypes of the four unique glutamine synthetase mutants in a murine model. Infect. Immun. *74*, 6491–6495.

Lee, W., VanderVen, B.C., Fahey, R.J., and Russell, D.G. (2013). Intracellular *Mycobacterium tuberculosis* exploits host-derived fatty acids to limit metabolic stress. J. Biol. Chem. *288*, 6788–6800.

Marrero, J., Rhee, K.Y., Schnappinger, D., Pethe, K., and Ehrt, S. (2010). Gluconeogenic carbon flow of tricarboxylic acid cycle intermediates is critical for *Mycobacterium tuberculosis* to establish and maintain infection. Proc. Natl. Acad. Sci. USA *107*, 9819–9824.

Martinez, F.O., Gordon, S., Locati, M., and Mantovani, A. (2006). Transcriptional profiling of the human monocyte-to-macrophage differentiation and polarization: new molecules and patterns of gene expression. J. Immunol. *177*, 7303–7311.

McAdam, R.A., Weisbrod, T.R., Martin, J., Scuderi, J.D., Brown, A.M., Cirillo, J.D., Bloom, B.R., and Jacobs, W.R., Jr. (1995). *In vivo* growth characteristics of leucine and methionine auxotrophic mutants of *Mycobacterium bovis* BCG generated by transposon mutagenesis. Infect. Immun. *63*, 1004–1012.

Muñoz-Elías, E.J., and McKinney, J.D. (2005). *Mycobacterium tuberculosis* isocitrate lyases 1 and 2 are jointly required for in vivo growth and virulence. Nat. Med. *11*, 638–644.

Pandey, A.K., and Sassetti, C.M. (2008). Mycobacterial persistence requires the utilization of host cholesterol. Proc. Natl. Acad. Sci. USA *105*, 4376–4380.

Pethe, K., Sequeira, P.C., Agarwalla, S., Rhee, K., Kuhen, K., Phong, W.Y., Patel, V., Beer, D., Walker, J.R., Duraiswamy, J., et al. (2010). A chemical genetic screen in *Mycobacterium tuberculosis* identifies carbon-source-dependent growth inhibitors devoid of in vivo efficacy. Nat. Commun. *1*, 57.

Riendeau, C.J., and Kornfeld, H. (2003). THP-1 cell apoptosis in response to Mycobacterial infection. Infect. Immun. *71*, 254–259.

Savvi, S., Warner, D.F., Kana, B.D., McKinney, J.D., Mizrahi, V., and Dawes, S.S. (2008). Functional characterization of a vitamin B12-dependent methylmalonyl pathway in *Mycobacterium tuberculosis*: implications for propionate metabolism during growth on fatty acids. J. Bacteriol. *190*, 3886–3895.

Sharma, S.K., and Mohan, A. (2006). Multidrug-resistant tuberculosis: a menace that threatens to destabilize tuberculosis control. Chest *130*, 261–272.

Simeone, R., Bobard, A., Lippmann, J., Bitter, W., Majlessi, L., Brosch, R., and Enninga, J. (2012). Phagosomal rupture by *Mycobacterium tuberculosis* results in toxicity and host cell death. PLoS Pathog. *8*, e1002507.

Singh, V., Jamwal, S., Jain, R., Verma, P., Gokhale, R., and Rao, K.V. (2012). *Mycobacterium tuberculosis*-driven targeted recalibration of macrophage lipid homeostasis promotes the foamy phenotype. Cell Host Microbe *12*, 669–681.

Singhal, A., Jaiswal, A., Arora, V.K., and Prasad, H.K. (2007). Modulation of gamma interferon receptor 1 by *Mycobacterium tuberculosis*: a potential immune response evasive mechanism. Infect. Immun. *75*, 2500–2510.

Smith, D.A., Parish, T., Stoker, N.G., and Bancroft, G.J. (2001). Characterization of auxotrophic mutants of *Mycobacterium tuberculosis* and their potential as vaccine candidates. Infect. Immun. *69*, 1142–1150.

Srinivasan, V., and Morowitz, H.J. (2006). Ancient genes in contemporary persistent microbial pathogens. Biol. Bull. *210*, 1–9.

Stewart, G.R., Patel, J., Robertson, B.D., Rae, A., and Young, D.B. (2005). Mycobacterial mutants with defective control of phagosomal acidification. PLoS Pathog. *1*, 269–278. http://dx.doi.org/10.1371/journal.ppat.0010033.

Tullius, M.V., Harth, G., and Horwitz, M.A. (2003). Glutamine synthetase GlnA1 is essential for growth of *Mycobacterium tuberculosis* in human THP-1 macrophages and guinea pigs. Infect. Immun. *71*, 3927–3936.

Velayati, A.A., Masjedi, M.R., Farnia, P., Tabarsi, P., Ghanavi, J., Ziazarifi, A.H., and Hoffner, S.E. (2009). Emergence of new forms of totally drug-resistant tuberculosis bacilli: super extensively drug-resistant tuberculosis or totally drug-resistant strains in iran. Chest *136*, 420–425.

Venugopal, A., Bryk, R., Shi, S., Rhee, K., Rath, P., Schnappinger, D., Ehrt, S., and Nathan, C. (2011). Virulence of *Mycobacterium tuberculosis* depends on lipoamide dehydrogenase, a member of three multienzyme complexes. Cell Host Microbe *9*, 21–31.

Watanabe, S., Zimmermann, M., Goodwin, M.B., Sauer, U., Barry, C.E., 3rd, and Boshoff, H.I. (2011). Fumarate reductase activity maintains an energized membrane in anaerobic *Mycobacterium tuberculosis*. PLoS Pathog. *7*, e1002287.

Weitzel, M., Nöh, K., Dalman, T., Niedenführ, S., Stute, B., and Wiechert, W. (2013). 13CFLUX2—high-performance software suite for (13)C-metabolic flux analysis. Bioinformatics *29*, 143–145.

Wiechert, W., Möllney, M., Petersen, S., and de Graaf, A.A. (2001). A universal framework for 13C metabolic flux analysis. Metab. Eng. *3*, 265–283.

World Health Organization. (2011). Tuberculosis fact sheet (Geneva, Switzerland: World Health Organization).